A Master's Thesis

Attenuation of the stem cell properties and the oxidative phosphorylation by ampelopsin in therapy-resistant MDA-MB-231 breast cancer cells

Vi Nguyen-Phuong Truong

Department of Interdisciplinary Graduate Program in

Advanced Convergence Technology and Science

Graduate School

Jeju National University

December 2021

Attenuation of the stem cell properties and the oxidative phosphorylation by ampelopsin in therapy-resistant MDA-MB-231 breast cancer cells.

Vi Nguyen-Phuong Truong

(Supervised by professor Somi Kim Cho)

A thesis submitted partial fulfilment of the requirement for the degree of Master of Interdisciplinary Graduate Program in Advanced Convergence Technology and Science

2022. 02

This thesis has been examined and approved.

손영숙

김소리

조솜미

Interdisciplinary Graduate Program in

Advanced Convergence Technology and Science

Graduate School

Jeju National University

치료 저항성 MDA-MB-231 유방암 세포에서 암펠롭신에 의한 줄기 세포 특성 및 산화적 인산화 억제

트렁 응웬 푸옹 비

지도교수 김소미

이 논문을 이학 석사학위 논문으로 제출함

2022년 2월

트렁 응웬 푸옹 비의 이학 석사학위 논문을 인준함

심사위원장 손영욱

위 원 김소미

위 원 조문제

제주대학교 대학원

2022년 2월

CONTENTS

ABSTRACT 1

1. INTRODUCTION 2

2. MATERIALS AND METHODS 6

2.1. Cell culture 6

2.2. Cell viability assay 6

2.3. Cell invasion assay 6

2.4. Wound healing assay 7

2.5. Mammosphere Formation Assay 7

2.6. Flow Cytometric Assay for $CD44^{+}/CD24^{-}$ Population 7

2.7. ALDEFLUOR Assay 8

2.8. Annexin V/propidium Iodide Staining 8

2.9. Colony Formation Assay 8

2.10. Real-Time Polymerase Chain Reaction (PCR) 8

2.11. Western blot analysis 9

2.12. XF Seahorse Analysis 9

2.13. Statistical Analysis 10

3. RESULTS 11

3.1. Ampelopsin shows anti-cancer effects in MDA-MB-231/IR Cells 11

3.2. Ampelopsin Attenuates Stemness Characteristics in MDA-MB-231/IR Cells 13

3.3. Ampelopsin Prevents the Invasive and Migratory Behavior by MDA-MB-231/IR Cells 15

3.4. Ampelopsin Regulates Glucose Metabolism by Reducing Oxidative Phosphorylation in MDA-MB-231/IR Cells 17

3.5. Ampelopsin Inhibits NF-κB signaling pathway of MDA-MB-231/IR Cells 20

4. DISCUSSION 24

5. CONCLUSIONS 29

SUPPLEMENTARY DATA.....30

REFERENCES.....33

LIST OF FIGURES

Fig. 1. The structure of ampelopsin.....5

Fig. 2. Ampelopsin causes cytotoxicity in MDA-MB-231/IR cells.....12

Fig. 3. The attenuation of ampelopsin on stemness properties of MDA-MB-231/IR cells ...14

Fig. 4. Ampelopsin prevents the invasion and migration of MDA-MB-231/IR cells.....16

Fig. 5. Ampelopsin impairs oxidative phosphorylation metabolism in MDA-MB-231/IR cells.....19

Fig. 6. Ampelopsin exerts the inhibitiory potential of NF-κB activity in MDA-MB-231/IR cells.....22

Fig. S1. Flavonoid compounds targets cell viability of MDA-MB-231 and MDA-MB-231/IR cells.....30

Fig. S2. The levels of AMPK, p-AMPK, mTOR and p-mTOR were evaluated in MDA-MB-231 and MDA-MB-231/IR cells.....31

LIST OF TABLES

Table S1. The sequences of primers for mitochondrial OXPHOS genes. 32

ABSTRACT

Cancer stem cells (CSCs) have an important function in tumorigenesis and therapy resistance. Therefore, targeting CSCs is a prominent therapeutic option for triple negative breast cancer (TNBC) treatment. Ampelopsin, a major substance found in *Ampelopsis* species, could prevent the proliferation, colony formation ability as well as trigger apoptosis at dose-dependent manners in resistant MDA-MB-231/IR cells that are enrichment of stem-like characteristics. Importantly, ampelopsin exerted the inhibitory ability on the stem cell profiling of MDA-MB-231/IR cells, as represented by the results of mammosphere formation, $CD44^{+}/CD24^{-}$ population, aldehyde dehydrogenase (ALDH) population and the levels of well-known stemness markers. Moreover, ampelopsin inhibited the epithelial–mesenchymal transition (EMT) transition, as evidenced by a dramatically reduction of migration, invasive capacity and the levels of mesenchymal markers – Snail, Slug and MMP2 and a rise of epithelial marker – E-cadherin. Notably, ampelopsin dramatically diminished oxidative phosphorylation which reflected mitochondrial function, as represented by a decrease of oxygen consumption rate and adenosine triphosphate level in resistant MDA-MB-231/IR cells. Interestingly, NF-κB signaling pathways was suppressed after ampelopsin treatment, displayed by the declines of IκBα and p65 phosphorylation, as well as the NF-κB activation stimulated by tumor necrosis factor (TNF)-α treatment. These findings illustrated that ampelopsin acts as a TNF-α/NF-κB axis inhibitor in breast cancer stem cells.

1. INTRODUCTION

Breast cancer is the most prevalent malignancy and leading cause of cancer death among women. Breast cancer cases also accounted for 24.5% of cancers cases in women, revealing the highest frequency in most countries worldwide, following the Global Cancer Statistics 2020 provided by the International Agency for Research on Cancer [1]. In an effort to get more effective treatment on patients, the classification of breast cancer has been identified. Triple negative breast cancer (TNBC) is defined as an extremely aggressive form of breast cancer that makes up nearly 15% of all aggressive breast cancer cases and it is related to the poor prognosis and metastatic occurrence of breast cancer patient. Due to the absence of the expression of estrogen receptor (ER), progesterone receptor (PR), and human epidermal growth factor receptor 2 (HER2), this group does not respond to hormonal therapies and currently limits efficiency therapy options [2]. In addition, TNBC also showed the chemotherapeutic resistance, increased risk of early metastasis, and recurrence. Thus, the development of TNBC treatment strategies is an urgent necessity in breast cancer patients [3].

In heterogeneous tumors, cancer stem cells (CSCs) are well-known as a tumor-initiating cells. Because of the existence of CSCs in quiescent and poorly differentiated cells within mammary tumor contribute to therapy resistance, tumor recurrence and metastasis, current potential therapies to eliminate breast cancer are failure. CSCs have a greater tumorigenic; therefore, they can form tumor when transplanted into mice at low numbers, while cancer cells cannot [4]. Several reports have illustrated the “gold standard” signatures estimating breast cancer stem cells (BCSCs) frequency, for example the population of $CD44^{+}/CD24^{-/low}$, the population of aldehyde dehydrogenasehigh ($ALDH^{high}$) or $CD133^{+}$ genotypes [5]. OCT4, STAT3, β-catenin, Sox2, Nanog, MYC, and KLF4, well-known pluripotent transcriptional factors, are involved in the biological process of CSCs growth. Furthermore, the enrichment

of multiple intracellular pathways in CSCs (e.g., SRC kinase, JAK-STAT, Notch, Wnt/β-catenin, mTOR, Hedgehog, TGF/SMAD, PI3K/AKT, and nuclear factor-κB [NF-κB]) are observed to support their self-renewal activity and proliferation [4,6]. In previous studies, we characterized a therapy-resistant MDA-MB-231/IR cell line established from parental TNBC breast cancer MDA-MB-231 cell line, that exhibited higher stemness features (e.g., low ROS levels, migration, invasive capacity, resistant to chemotherapeutic drugs and radiotherapy). In addition, enrichment of TNF-α, NF-κB signaling, and Toll-like receptors pathway were examined in this cell line by transcriptome profiling [7,8].

Metabolic status has been identified as a specific hallmark of CSCs [9]. In comparison to cancer cells, CSCs respond differently to energy demands for maintenance of their homeostasis. Cancer cells use glycolysis to produce lactate and allows the diversion of glycolytic intermediates into various biosynthesis pathways to support their devopment even in the presence of oxygen. This state of energy production is designed as the Warburg effect or aerobic glycolysis [10]. In contrast, CSCs show a variable metabolic imprint that allows them to switch between glycolysis and oxidative phosphorylation (OXPHOS) metabolism to promote tumor formation and maintain homeostasis [9]. In addition, accumulating evidence has demonstrated that the increased OXPHOS metabolic phenotype in CSCs facilitates the enrichment of their stem cell features, metastatic ability, invasiveness, greater tumorigenic capacity, while enhancing their DNA damage resistance [11,12]. Moreover, stimulation of OXPHOS phenotype is controlled by metabolic pathway that is dependent on NF-κB to promote the proliferation of cancer cells as previous study [13]. Therefore, the OXPHOS inhibitor has emerged as a promising therapeutic target for cancer treatment approach [14].

The transcription factor NF-κB can control numerous genes regulating for proliferation, oncogenesis, cellular transformation, and metastasis features in breast cancer and stem-like cells [15,16]. NF-κB is defined as an important family consists five members: cREL, p65

(RELA), RELB, p100/p52, and p105/p50. These members share a conserved amino terminal Rel homology domain which supports DNA binding, nuclear localization, homo- and heterodimerization. Among NF-κB family, only p65, RELB, cREL has transactivation activation domains (TAD) which is crucial for transcriptional activity. In resting state, the NF-κB dimers are remained as an inactive complex with the IκB inhibitory proteins in the cytoplasm that delays nuclear import. The canonical and non-canonical pathways are both correlated to the activation of NF-κB signaling. In the canonical pathway with the participation of members have TAD domain, upon many stimuli (e.g., lipopolysaccharide – LPS, tumor necrosis factor – TNF or interleukin - IL) will activate the κB kinase (IKKs) inhibitor complex, causing phosphorylation of IκBs, leading to its ubiquitination and degradation. p65 is an important regulator of NF-κB activation, making it becomes an attractive target for drug development [15,17]. Y Gao et al. found the molecular connection between inflammatory and breast cancer metastasis via TNF-α-IKK-YAP/p65-HK2 signaling axis [18]. Furthermore, the upregulation of p65 reduces the inhibitory effect induced by celecoxib treatment in breast cancer [19]. The expression of p65 undergoes several post-translational modifications, especially phosphorylate at S536 and S276 residues can promote to tumorigenesis [20,21].

In recent studies, anticancer agents have been discovered in various phytochemicals isolated from medicinal plants species [22]. Ampelopsin which identified as dihydromyricetin, is a primary flavonoid found in various plants including a Chinese Rattan tea (Ampelopsis grossedentata) and a Japanese raisin tree (Hovenia dulcis Thunb.) [23-25]. Because of its beneficial activities, several methods have been developed to extract ampelopsin as well as various studies on the structure identification and its extensive biological functions [25]. Accordingly, ampelopsin is shown to modulate effectively various signaling in different cancers, including apoptosis promotion, anti-proliferation and

metastatic inhibition via ERK1/2, JNK pathway, PI3K/Akt or mTOR [26]. Subsequently, ampelopsin significantly improved paclitaxel and doxorubicin sensitivity in ovarian cancer cells [27]. Furthermore, accumulating studies have been showed that ampelopsin acts as a potential therapeutic agent in multiple metabolic diseases, such as in diabetes, obesity or non-alcoholic fatty liver disease [25,28]. Nevertheless, little is known about its impact on CSCs population, and the function of ampelopsin on the glucose metabolism has not been investigated yet in BCSCs. In reccent study, we investigated ampelopsin as a therapeutic potential agent in regulating the stemness characteristic and mitochondria function in triple negative radio- and chemo-resistant MDA-MB-231/IR breast cancer cells.

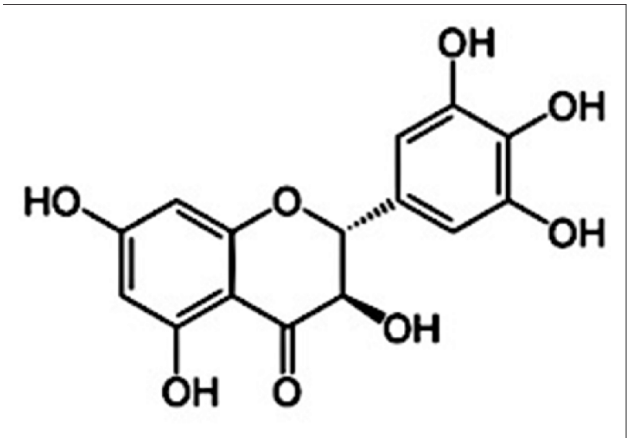

Fig. 1. The structure of ampelopsin

2. MATERIALS AND METHODS

2.1. Cell culture

The TNBC MDA-MB-231 cells (ATCC, Rockville, MD, USA) were used to establish a radio- and chemo-resistant MDA-MB-231/IR cells reported in previous study [7]. The fibroblast cells were a gift from Professor Moonjae Cho. MDA-MB-231, MDA-MB-231/IR and fibroblast cells were cultured in Dulbecco's Modified Eagle Medium DMEM (GIBCO, Carlsbad, CA, USA) supplemented with 10% heat-inactivated fetal bovine serum (FBS, GIBCO, Carlsbad, CA, USA) and 1% antibiotic-antimycotic reagents (GIBCO). MCF-10A was cultured base on the recommendation from ATCC (Rockville, MD, USA). All cells were incubated at 37 °C under 5% CO2 atmosphere.

2.2. Cell viability assay

Cell viability was accessed by using MTT solution (3-(4,5-Dimethylthiazol-2-yl)-2,5-Diphenyltetrazolium Bromide) as previous described [29]. Briefly, 2×10^4 cells/mL were loaded into 96-well plates and then exposed with ampelopsin (TCI, Tokyo, Japan) at increasing concentrations. After different times of incubation, 100 μL MTT reagent (1 mg/mL) was supplemented and incubate for 2–3 hours at 37 °C. Then, the formazan crystals were dissolved in 150 μL of dimethyl sulfoxide (DMSO) for 30 minutes. The absorbance was measured at 570 nm by using a microplate reader (Tecan Group, Ltd., Salzburg, Austria). The rate of cell viability was calculated by the formula (control group − treated group) ÷ control group) × 100 %.

2.3. Cell invasion assay

The 24-well transwell plates (Corning, Cambridge, MA, USA) were used for the cell invasion assay as described previously [29]. Following the instructions of manufacturer, 1% matrigel was applied to coat the upper chambers until the gel had solidified completely. After that, 2×10^5 cells/well in DMEM-free FBS supplemented with ampelopsin (dosage at 0 and

12.5 μM) were loaded into each well. The lower chambers were added with DMEM containing 10% FBS. Following incubation for 24 hours, 4% paraformaldehyde was used to fix the migratory cells. Further, these cells were stained in crystal violet and washed by PBS 1X to discard the detached violet dyes. Subsequently, a phase-contrast microscope was used to access the stain cells.

2.4. Wound healing assay

Cells (2 × 105 cells/mL) were loaded into six-well plates. When the cell density reached 90-95% confluence, a 200 μL sterile pipette tip was used to make an equal scratch wound and then each well was rinsed with PBS 1X to remove the detached cells. After that, the cells were treated with or without ampelopsin following exposure for 24 hours. The wound areas were observed under an inverted phase-contrast microscope.

2.5. Mammosphere Formation Assay

The ultralow attachment dishes were used to seed 2×10^4 single cells/mL. The cells were culture in complete MammoCult Human Medium (Stemcell Technologies, Vancouver, BC, Canada) and then exposed with ampelopsin at dosages 0, 25, 50, and 100 μM. A phase-contrast microscope was used to observe mammospheres (size > 60 μm) after 10 days of incubation.

2.6. Flow Cytometric Assay for $CD44^+/CD24^-$ Population

Cells (1×10^5 cells/mL) were seeded and then treated with increasing concentrations of ampelopsin at 0, 25, 50, and 100 μM. After exposure for 24 hours, cells were suspended in immunofluorescence staining buffer containing anti-human CD24 antibody conjugated with phytoerythrin (PE) and anti-human CD44 antibody conjugated with fluorescein isothiocyanate (FITC) (BD Pharmingen, San Diego, CA, USA). After incubation for 15 minutes at 4°C, the $CD44^+/CD24^{-/low}$ population was detected by fluorescence-activated cell sorting (FACSCalibur, Becton Dickinson, Franklin Lakes, NJ, USA).

2.7. ALDEFLUOR Assay

An Aldefluor assay kit (Stemcell Technologies) was utilized to access the activity of ALDH enzyme as described previously [29]. Briefly, 1×10^5 cells/mL were loaded and then treated with or without ampelopsin. After 24-hour incubation, Aldefluor assay kit was applied following the manufacturer's instructions. The ALDH population were identified by FACSCalibur flow cytometer. 4-diethylaminobenzaldehyde (DEAB), an ALDH inhibitor, was introduced as a negative control.

2.8. Annexin V/propidium Iodide Staining

Cells (1×10^5 cells/mL) were seeded onto 60 mm plates and exposed with increasing concentration of ampelopsin. After that, cells were rinsed with PBS and collected. The Annexin V-FITC Apoptosis Detection Kit (BD Pharmingen) was used to detect the apoptotic population for 15 minutes at 37 °C. The apoptotic cells were measured by using FACSCalibur flow cytometer.

2.9. Colony Formation Assay

The single cells (400 cells/mL) were loaded onto 60 mm plates and then treated with increasing dosages of ampelopsin. After 10 days for incubation, PBS was used to wash cells following fixing cells with 4% paraformaldehyde. After that, cells were stained with crystal violet for 30 minutes. The number of colonies were counted by using the ImageJ software (NIH, Bethesda, MD, USA).

2.10. Real-Time Polymerase Chain Reaction (PCR)

Cells (1×10^5 cells/mL) were seeded into 60 mm plates and then exposed with ampelopsin at dosages 0, 50, and 100 μM for 24 hours. Suspension cells were collected by trypsin. Total RNA was extracted using TRIzol reagent (Invitrogen, Carlsbad, CA, USA) and reversed by the ImProm-II™ Reverse Transcription System kit (Promega, Madison, Wisconsin, USA). After that, quantitative real-time PCR was conducted by TOPreal™ qPCR

2× PreMIX kit (Enzynomics, Daejeon, South Korea). The gene expression was accessed by the $2^{-\Delta\Delta Ct}$ method as reported by Livak and Schmittgen [30]. The primers used for real-time PCR are listed in Table S1.

2.11. Western blot analysis

Western blotting experiment was described as previous studies [31]. The cells were seeded and treated with increasing concentration of ampelopsin. Following 24 hour-incubation, cell lysates were extracted using the radioimmunoprecipitation assay (RIPA) buffer, protease inhibitor and phenylmethanesulfornyl fluoride solution – PMSF (Sigma-Aldrich, Missouri, USA). Then, a bicinchoninic acid (BCA) protein assay kit (Thermo Fisher Scientific, Waltham, MA, USA) was used to measure protein concentration. After that, 20–40 µg of protein was loaded and separated by sodium dodecyl sulfate-polyacrylamide gel electrophoresis (SDS-PAGE). Subsequently, the gels were electrophoretically transferred to polyvinylidenefluoride (PVDF) membranes following by blocking with skim milk. The membranes were incubated with primary antibodies which purchased from Cell Signaling Technology, Beverly, MA, USA and BD Transduction Laboratories, San Jose, CA, USA (the mouse anti-β-catenin and E-cadherin antibody). Almost primary antibodies were diluted at 1:1000, except the anti-GAPDH primary antibody was diluted at 1:10000. After incubation at 4^0C overnight, the membranes were washed with Tris Buffered Saline-Tween® 20 (TTBS), following exposing with the secondary antibodies (Vector Laboratories, Burlingame, CA, USA) which diluted at 1:5000. A ECL Plus kit (Biosesang, Seongnam, South Korea) was used to detect target bands.

2.12. XF Seahorse Analysis

A Seahorse XF cell mitochondria stress test kit provided by XF24 Extracellular Flux Analyzer (Seahorse Bioscience, Agilent Technologies, CA, USA) was used to measure the oxygen consumption rate (OCR). 10^4 cells/well were loaded in Seahorse XF24 24-well plates.

Cells were then treated with or without ampelopsin (50 and 100 μM) for 24 hours. Subsequently, the old medium was changed with warmed XF Assay Base Medium measured at pH 7.4 and added with 1 mM sodium pyruvate, 10 mM glucose, and 2 mM l-glutamine. After that, cells were incubated for 1 hour at 37 °C in a CO_2-free incubator. The cells were then subsequently sequential treated with oligomycin (2 μM), carbonyl cyanide-p trifluoromethoxyphenylhydrazone (1 μM), and rotenone (1 μM)/antimycin A (2 μM). The OCR values was shown in pmol/min.

2.13. Statistical Analysis

The data were analyzed by GraphPad Prism 8.0 software (La Jolla, CA, USA). Data are presented as means ± standard deviations of triplicate independent experiments. Student's t-test was used to access differences between two sets of data. * $p < 0.05$ was considered as statistical significance.

3. RESULTS

3.1. Ampelopsin shows anti-cancer effects in MDA-MB-231/IR Cells

When compared to parental cells, MDA-MB-231/IR cells exhibited greater radio- and chemo-resistant characteristic [7]. Therefore, screening phytochemicals targeting MDA-MB-231/IR are performed. Among several flavonoids have been found as anticancer agents against breast cancer [32-37], ampelopsin provided the most potential agent against resistant MDA-MB-231/IR cells out of all the phytochemicals studied (Fig. S1). In addition, Fig. 1A showed that ampelopsin exhibited a greater cytotoxicity on MDA-MB-231/IR cells, as determined by IC50 58 ± 3.84 μM vs. IC50 42.89 ± 1.86 μM after 24 hours of incubation. As a result, ampelopsin was chosen for additional research on MDA-MB-231/IR cells. Ampelopsin was also non-cytotoxic to normal fibroblast cells and normal breast cells MCF-10A, demonstrating that it was harmless to normal human cell lines. Notably, a dramatic reduction of colony number at concentration of 6.25 μM (75% ± 7.71%) and 12.5 μM (12.8% ± 9.7%), and no colonies at higher dosages were observed after ampelopsin treatment for 10 days on MDA-MB-231/IR cells (Fig. 1B). Moreover, we determined whether ampelopsin could enhance apoptosis in resistant cells. In Fig. 1C, at a dosage of 50 μM and 100 μM, ampelopsin induced the percentage of apoptotic cells by 13.47% ± 4.66% and 18.2% ± 1.08%, as revealed by annexin V/PI. Moreover, ampelopsin-exposed MDA-MB-231/IR cells showed a drop in the levels of caspase 3 (0.28 ± 0.16-fold) and caspase 7 (0.38 ± 0.23-fold). Furthermore, the cleavage of poly (ADP-ribose) polymerase (PARP), an essential substrate of caspase cascade, was allegedly necessary for apoptosis in several cell types [38,39]. The stem cell population in non-small cell lung cancer (NSCLC) displayed reduced apoptosis following treatment with cisplatin, as evidenced by decreased the cleavage form of PARP and the activation of caspase 3 [40]. Fig. 1D showed that ampelopsin dramatically declined the PARP level and increased the level of cleaved fragment, as shown by a growth of c-

PARP/PARP, as evidenced by 2.55 ± 0.39 and 4.24 ± 0.73-fold at 50 μM and 100 μM, in comparison to control.

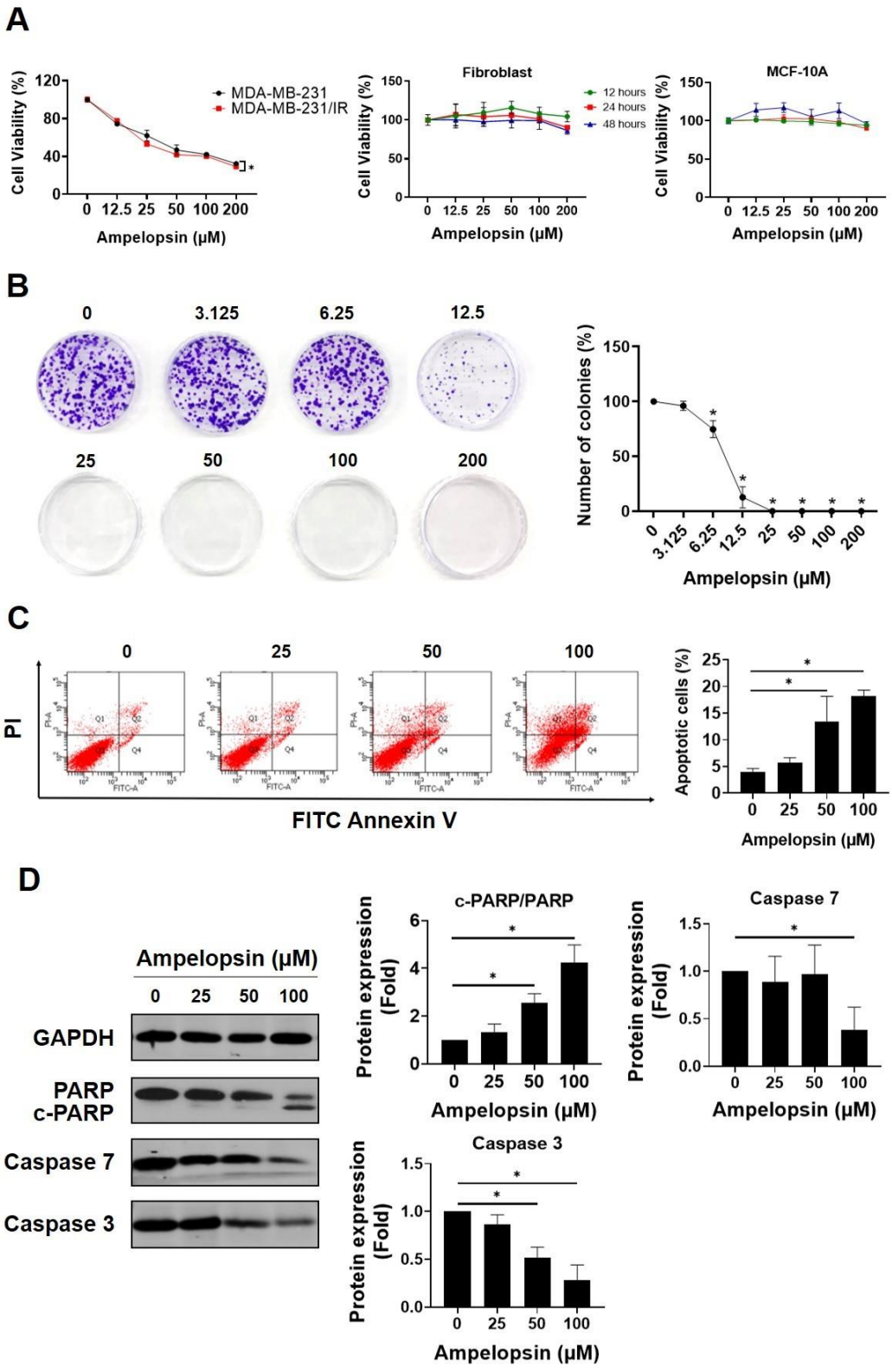

Fig. 2. Ampelopsin causes cytotoxicity in MDA-MB-231/IR cells.

The cell viability of MDA-MB-231, MDA-MB-231/IR cells, fibroblast cells as well as MCF-10A were determined by MTT assay following ampelopsin incubation for 24 hours. (B) After 10 days of ampelopsin exposure, the number of colonies were calculated. (C) Following treatment with ampelopsin for 24 hours, FACS analysis was used to evaluate the apoptotic population using annexin V/PI staining. (D) Apoptosis markers were analyzed by Western blotting after ampelopsin treatment for 24 hours. GAPDH was considered as the loading control.

3.2. Ampelopsin Attenuates Stemness Characteristics in MDA-MB-231/IR Cells

Since MDA-MB-231/IR cells apparently show higher stem cell-like profiles, displayed by increased mamosphere numbers, migrated and invasive capacity, stemness markers or low ROS levels than parental cells [7,8] , we investigated whether ampelopsin could suppress the stemness traits of resistant cells. The spheroid formation capacity is correlated to the self-renewal capability of CSCs, promoting increased tumor growth, recurrence, metastasis and stem cell survival [41]. In this result, after 10 days of treatment in different concentration (0, 25, 50, and 100 μM), ampelopsin rapidly reduced mammospheres generation in resistant cells, as seen in Fig. 2A. Furthermore, FACS analysis revealed that $CD44^{+}/CD24^{-/low}$ phenotype, a specific subpopulation of breast CSCs, reduced after ampelopsin treatment (0.336% ± 0.171%) (Fig. 2B). Subsequently, at non-lethal dosage at 12.5 μM, ampelopsin reduced the ALDH-positive cells, which were previously reported as a stemness signature [5], to 0.4% (2.5-fold) (Fig. 2C). Surprisingly, a dose-dependent reduction of common CSC markers, MRP1 (0.55 ± 0.03-fold), CD44 (0.48 ± 0.03-fold), KLF4 (0.47 ± 0.11-fold) and β-catenin (0.49 ± 0.18-fold) were observed in western blot experiment revealed after 100 μM ampelopsin treatment. According to these findings, ampelopsin successfully decreased the stem-like behaviors in MDA-MB-231/IR cells.

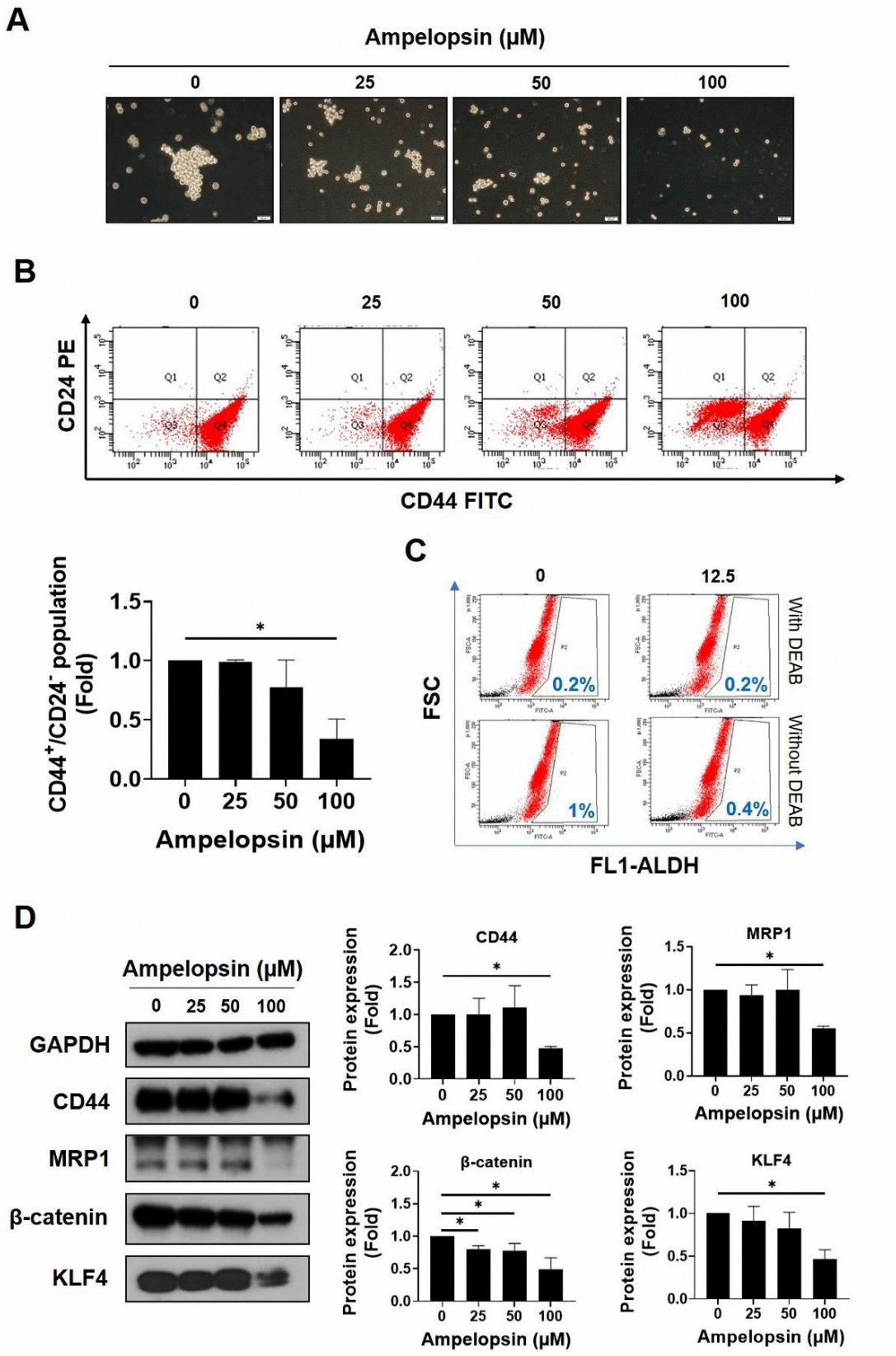

Fig. 3. The attenuation of ampelopsin on stemness properties of MDA-MB-231/IR cells

(A) Mammosphere were observed after ampelopsin treatment for 10 days at 100× magnification under microscope. (B) The CD44+/CD24−/low population was determined by FACS analysis after 24 hours treatment of ampelopsin. (C) The Aldefluor assay test kit was used to measure $ALDH^+$ population following ampelopsin. DEAB was served as a negative control. (D) Stemness markers were analyzed by western blotting experiment following a 24-hour ampelopsin incubation. The loading control was GAPDH.

3.3. Ampelopsin Prevents the Invasive and Migratory Behavior by MDA-MB-231/IR Cells

The epithelial–mesenchymal transition (EMT) confers malignant features to cancer cells, including enhanced cancer stem cell activity, metastatic ability, therapy resistance and immune clearance [42]. Consequently, we investigated the effects of ampelopsin on invasive capacity and migration by resistant cells. In Fig. 3A, ampelopsin reduced dose-dependently the migrated cells after 24-hour exposure at non-lethal dosages, represented by a wound healing experiment. Furthermore, transwell plates were used to access the invasive cell by the cell invasion assay. A reduce of invasive ability by 57.7% ± 0.47% was observed when exposed cells with ampelopsin (Fig. 3B). In addition, the levels of common EMT markers were accessed by western blotting. As we expected, ampelopsin significantly decreased the levels of the mesenchymal markers, Slug, Snail and MMP2 at non-lethal dosages, reaching 0.59 ± 0.16, 0.62 ± 0.08-fold and 0.64 ± 0.17-fold, respectively. Furthermore, Fig. 3C showed that ampelopsin significantly increased the level of E-cadherin, an epithelial marker. These data illustrated the crucial function of ampelopsin on suppression of EMT transition of MDA-MB-231/IR cells.

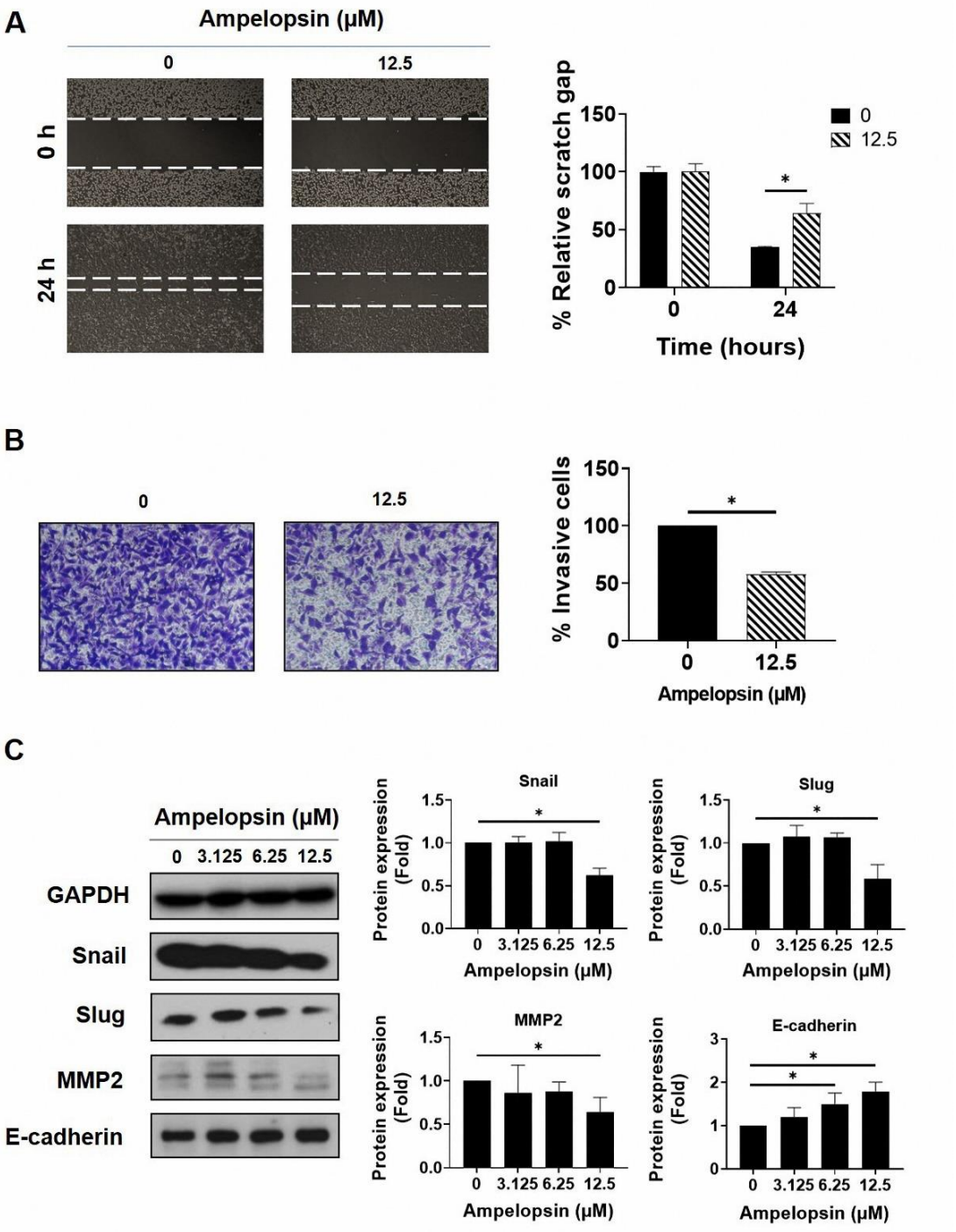

Fig. 4. Ampelopsin prevents the invasion and migration of MDA-MB-231/IR cells

(A) Following 24 hours treatment with ampelosin at dose 12.5 μM, the migrated cells were accessed by performing the wound healing assay. A phase-contrast microscopy was used to capture the images at 100× magnification. (B) Invasive cells after 24 hours ampelopsin treatment was calculated by the cell invasion assay. A phase-contrast microscopy was used to capture the images at 100× magnification. (C) Western blotting analysis was performed to

access the levels of mesenchymal and epithelial markers following treatment with ampelopsin for 24 hours. GAPDH was considered as the loading control.

3.4. Ampelopsin Regulates Glucose Metabolism by Reducing Oxidative Phosphorylation in MDA-MB-231/IR Cells

Current reports have demonstrated that CSCs exacerbated on oxidative phosphorylation rather than cancer cells to enhance their stemness characteristic and confer to resistance against chemotherapy, thus the suppression of OXPHOS in CSCs can be a potential target in cancer therapy [9,14]. Ampelopsin has been previously reported to ameliorate the cellular damage and improve metabolic diseases by modulating various signaling pathways correlated to glucose metabolism [28]. However, the regulations of ampelopsin on glucose metabolism in CSCs are still largely unknown. Interestingly, it was a 0.56 ± 0.12-fold decreased levels of AMPK phosphorylation and a 1.5 ± 0.16-fold enhanced levels of mTOR phosphorylation, a well-known downstream of AMPK in MDA-MB-231/IR cells in comparison to their parent cells (Fig. S2). Interestingly, Fig. 4A showed that ampelopsin treatment activated AMPK signaling pathway by increasing the level of AMPK phosphorylation by 2.0 ± 0.13-fold, while it reduced the levels of the phosphorylation of mTOR (0.52 ± 0.13-fold). Due to ampelopsin could modulate the activation of AMPK and the suppression of mTOR, we tested whether ampelopsin could regulate glucose metabolism in therapy-resistant cells. In Fig. 4B, ampelopsin could decrease the oxygen consumption rate (OCR), which is previous reported to reflect the OXPHOS metabolism or mitochondrial respiration [43]. According to the levels of OCR, 100 μM ampelopsin impaired mitochondria metabolism, represented by the reduce the of basal respiration (46.4% ± 2.31%), maximum respiration (79.2% ± 7.99%) and adenosine triphosphate (ATP) production (31.6% ± 1.15%). In addition, by performing real-time PCR, Fig. 4C showed that ampelopsin treatment reduced steeply the gene expression related to OXPHOS metabolism as listed: *NDUFA10* – NADH:ubiquinone oxidoreductase

subunit A10, *SDHB* - succinate dehydrogenase complex subunit B, *COX5B* - cytochrome c oxidase subunit 5B, *COX4I1* - cytochrome C oxidase subunit 4 isoform 1, *ATP5G3* - ATP synthase membrane subunit C3, *SCO2* - synthesis of cytochrome C oxidase 2, *CYC1* - cytochrome C1, *UQCRC1* - ubiquinol-cytochrome C reductase core protein 1, *PPARGC1A* - peroxisome proliferator-activated receptor-gamma coactivator 1-alpha and *ATP5B* - ATP synthase F1 subunit beta. According to these results, ampelopsin can have a vital function in OXPHOS inhibition of MDA-MB-231/IR cells.

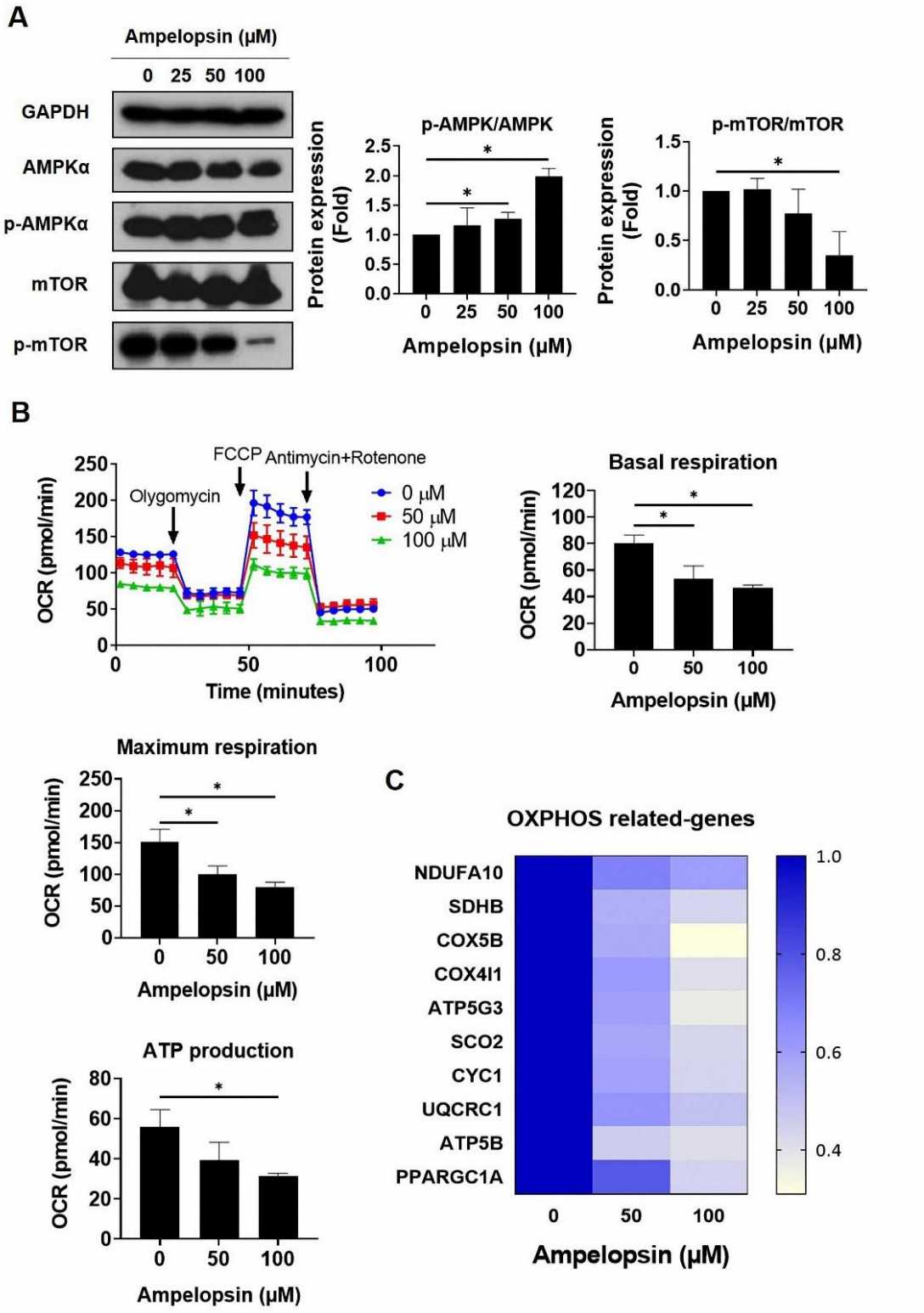

Fig. 5. Ampelopsin impairs oxidative phosphorylation metabolism in MDA-MB-231/IR cells.

(A) Western blotting analysis showed the levels of AMPKα, p-AMPKα, mTOR, and p-mTOR after 24 hours incubation with ampelopsin. (B) The levels of OCR, basal respiration, ATP production, and maximum respiration were accessed by XF Seahorse analysis after ampelopsin treatment for 24 hours. Cells were exposed with XF assay medium supplemented with pyruvate (1 mM), glucose (10 mM), and l-glutamine (2 mM), and then treated with oligomycin (2 μM), carbonyl cyanide-p trifluoromethoxyphenylhydrazone (1 μM), antimycin (1 μM), and rotenone (1 μM). (C) The gene expression was analyzed by real-time PCR. GAPDH was considered as the loading control.

3.5. Ampelopsin Inhibits NF-κB signaling pathway of MDA-MB-231/IR Cells

The elevated of NF-κB activity has been reported in many tumor types. When activated, the transcription factor NF-κB controls a number of target genes implicated in cancer development, metastasis and chemoresistance [16]. Furthermore, p65, a vital member of transcriptional activity of NF-κB family, reportedly acts as a physiological regulator of metabolic alteration by stimulating oxidative phosphorylation in normal and cancer cells [13]. Due to the importance of NF-κB activation in tumor growth and the enrichment of NF-κB signaling in MDA-MB-231/IR cells, as evidenced by the transcriptomic analysis from previous study [7], we investigated whether ampelopsin could diminish NF-κB activity in resistant cells. Notably, the levels of ratio of p-IκBα/IκBα (6.13 ± 0.90-fold) and p-p65/p65 (7.82 ± 1.55-fold) were significantly elevated compared to parental cells (Fig. 5A). In addition, Fig. 5B showed that ampelopsin markedly reduced the levels of p-IκBα/IκBα (0.22 ± 0.06-fold) and p-p65/p65 (0.05 ± 0.02-fold) compared with untreated controls. To clarify the mechanism of ampelopsin on NF-κB activity, we also checked whether ampelopsin may inhibit TNF-activated NF-κB activity, as the TNF-α/NF-κB axis is reported to promote tumor formation migration, invasion and angiogenesis in cancer [44]. Fig. 5C demonstrated that TNF-α treatment dramatically enhanced the levels of ratios of p-IκBα/IκBα (3.88 ± 0.72-fold) and p-p65/p65 (1.57 ± 0.35-fold), while simultaneously reducing IκB level. Notably,

ampelopsin could prevent the TNF-α-enhanced NF-κB activity by diminishing the levels of p-IκBα/IκBα (0.39 ± 0.07-fold) and p-p65/p65 (0.04 ± 0.01-fold) when pre-treated with TNF-α before 12 hours. These findings showed that the inhibitory potential of ampelopsin targeting NF-κB signaling stimulated by TNF-α, suggesting a novel role for ampelopsin as a TNF-α/NF-κB signaling inhibitor in BCSCs.

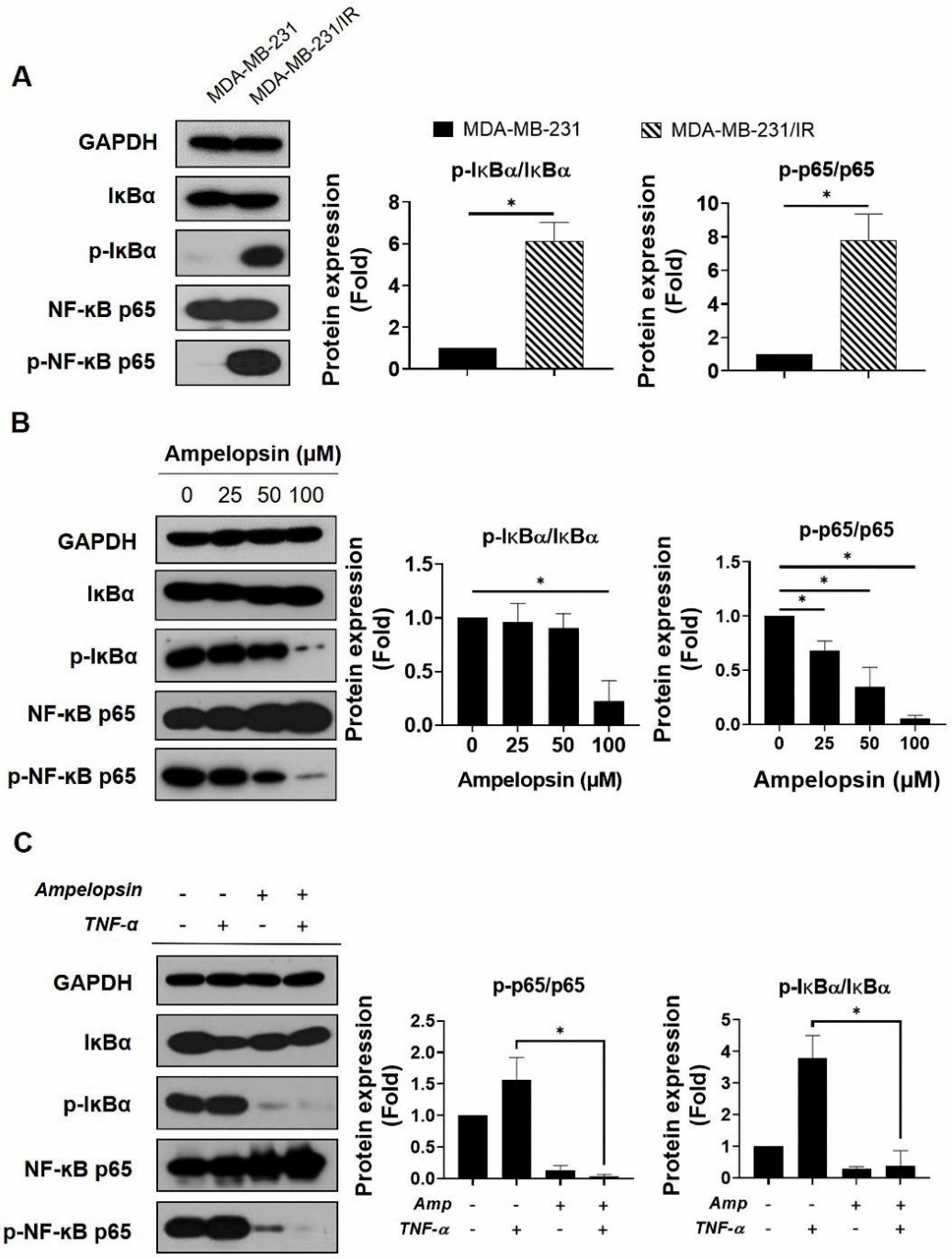

Fig. 6. Ampelopsin exerts the inhibitiory potential of NF-κB activity in MDA-MB-231/IR cells.

Western blotting experiments demonstrate (A) the levels of IκBα, p-IκBα, p65, and p-p65 compared to two cell line; (B) the levels of IκBα, p-IκBα, p65, and p-p65 in MDA-MB-231/IR cells after 24 hours treatment with ampelopsin; and (C) the TNF-α-enhanced NF-κB

signaling. In this experiment, cells were pretreated with 100 μM ampelopsin before being exposed to 10 ng/mL TNF-α for 12 hours. GAPDH was considered as the loading control.

4. DISCUSSION

CSCs have been identified as one of critical factors contribute tumor development, therapy resistance, and metastasis. Therefore, suppression of CSC population for cancer therapeutic strategy is a challenge. The subtype of breast cancer, TNBC displays heterogeneity, highly aggressiveness, and stemness features that contribute higher risk of early metastasis and therapeutic resistance in patients. Therefore, TNBC lacks of effective therapy options compared to other subtypes in breast cancer classification [4]. In previous studies, we established a specific therapeutic resistant TNBC MDA-MB-231 cell line, named as MDA-MB-231/IR cells which displayed enhanced stem cell-like characteristics, therapy resistance and distinct profile compared with the parental cells [7,8]. As a result, these resistant cells could be used in promising phytochemicals screening for novel chemotherapeutic compound for TNBC treatment. In Fig. S1, among several previous reported flavonoids as anti-cancer agents, we determined that ampelopsin, an effective phytochemical found in a traditional Chinese herb *Ampelopsis grossedentata,* displayed a greater cytotoxicity on MDA-MB-231/IR cells than on the parental cells. Moreover, ampelopsin is reported to induce apoptosis and autophagy in a variety of cancer cell lines [27,45,46]. This is the first research to examine ampelopsin acts as an apoptosis promoter in resistant cells and can play an important role for TNBC treatment. Indeed, ampelopsin treatment eliminated the CSC features by reducing the $CD44^{+}/CD24^{-/low}$ population, mammospheres, ALDH-positive cells, KLF4 level (an oncogene of maintenance breast CSC [47]), and β-catenin level (a transcriptional regulator for numerous CSC genes [48]) (Fig. 2).

The induction of EMT tends to lead the increase of the expression of genes involved in CSC phenotype in several tumor types to metastasize to distal organs, accompanied by the rise of mammosphere formation, colonies in soft agar and tumorigenicity in mice model [42]. During the EMT process, epithelial cells was lost the expression of some tight junction

molecules like E-cadherin and promote the mesenchymal transition, enhance migration, invasion and apoptosis evasion. Some transcription factor family such as Zeb, Snail and Twist initiate the EMT program [49]. In this study, ampelopsin treatment suppressed the migrated and invasive capability of MDA-MB-231/IR cells. Moreover, the levels of Snail, Slug and matrix metalloproteinases 2 - MMP2, widely have been used as mesenchymal markers were decreased as well as the level of epithelial marker E-cadherin was increased following ampelopsin treatment, indicating that ampelopsin can modulate the EMT transition in resistant cells.

AMPK, a crucial master mediator of energy balance, can govern cellular energy homeostasis and increase ATP generation to adapt with extracellular changes in environment. Interestingly, previous reports showed that AMPK activation is emerging as a metabolic tumor suppressor for cancer treatment [50]. Furthermore, the activation of AMPK can attenuate the activation of NF-κB signaling by preventing the translocation of p65 to the nucleus in activated macrophages in inflamed skin tissues [51]. An important downstream target of AMPK, mTOR, is reported to modulate autophagy in the presence of nutrients for tumor growth, as well as promotion of cell proliferation, protein synthesis and other cellular processes [50]. In non-small cell lung cancer, cell proliferation and cell growth was suppressed by the LKB1/AMPK axis via negatively regulation of mTOR activity [52]. Despite ampelopsin has been used to treat a variety of metabolic diseases and shown as an AMPK activator in previous studies [25,53], its effects in BCSCs have never been documented. In recent study, ampelopsin could enhance AMPK activation and decreased mTOR phosphorylation as shown in Fig. 4A. These findings indicated that ampelopsin may act as a metabolic regulator capable of CSC features suppression in MDA-MB-231/IR cells, motivating us to design further research to investigate how ampelopsin affects glucose metabolism in resistant cells.

There is growing reports that CSCs display elevated OXPHOS metabolism and enhanced ATP generation, which support their migration to a new metastasis site after dissociation from the basement membrane in tumor tissues. Furthermore, increased mitochondrial oxidative phenotype is necessary in the maintenance CSCs' biological behaviors including metastatic capacity, evasion of apoptosis, chemoresistance, self-renewal properties, and stemness characteristic [9,12]. Therefore, interfering the inhibition of OXPHOS metabolism or mitochondrial respiration is considered for elimination of CSC population [14]. Following previous reports, we examined whether ampelopsin is considered as a metabolic mediator to regulate the CSC population in MDA-MB-231/IR cells.

The oxygen consumption rate (OCR) was used as a mitochondrial OXPHOS indicator and showed to accurately reflect mitochondrial activity [43]. A recent research illustrated that LW1564, an inhibitor of HIF1-α, could impair cell growth in hepatocellular carcinoma by diminishing OCR levels and electron transport chain complex I, which lowered ATP generation and increased HIF-1α degradation. Subsequently, the ratio of AMP/ATP increased while the total ATP was reduced, resulting the activation of AMPK and downregulated mTOR signaling, inhibiting lipid synthesis [54]. Interestingly, MDA-MB-231/IR cells showed declines of OCR level, basal respiration, maximum respiration, as well as ATP production after ampelopsin introduction (Fig. 4B), indicating that ampelopsin plays a key role in preferentially attenuating the CSC population, that is rely on mitochondrial metabolism for proliferation and development. Furthermore, *PPARGC1A*, a gene that codes for PGC1-α protein, shown as an OXPHOS metabolic modulator, was considerably upregulated in tumor cells, and its attenuation greatly decreased the stemness characteristics of CSCs [11,12]. In our observation, Fig. 4C showed ampelopsin declined the expression of *PPARGC1A*, developing the potential therapeutic agent of ampelopsin on mitochondrial activity and ATP generation, preventing the proliferation of MDA-MB-231/IR cells.

The NF-κB transcriptional regulator drives the expression of several oncogenes that regulate apoptosis evasion, chemotherapy resistance, invasive, and metastasis in CSCs [15,16]. The NF-κB signaling has been reportedly controlled by the phosphorylation of NF-κB subunits and the mechanism that how they aid cancer growth are still being discovered [55]. Subsequently, the increased transcriptional activity of NF-κB and the regulation of NF-κB-directed transactivation has been controlled by p65 phosphorylation, an important member of NF-κB family [21,56]. Overexpression of NF-κB p65 facilitates EMT transition, leading the reduction of E-cadherin and desmoplakin, while increase the expression of mesenchymal markers, such as vimentin [15]. In recent study, western blot experiment showed that MDA-MB-231/IR cells enriched phosphorylation of IκB and p65 in comparison to MDA-MB-231 cells (Fig. 5A). This indicated that inhibiting NF-κB activity in breast CSCs might be beneficial therapeutically. Recent research has illustrated a vital role of NF-κB in modulation metabolic reprogramming in cancer. NF-κB was considered as an oncogenic mitochondria regulator; p65 induced mitochondria metabolism by increasing the expression of *SCO2* gene [13,57]. In recent study, ampelopsin could decrease the expression of *SCO2* (Fig. 4C), indicating that ampelopsin may diminish mitochondrial activity in MDA-MB-231/IR through inhibiting NF-κB. Notably, ampelopsin also dramatically suppressed NF-κB pathway, as evidenced by the reduction of IκBα and p65 phosphorylation (Fig. 5B). Previous study showed that TNF-α, a key pro-inflammatory cytokine, promotes the IKK phosphorylation and modulates the phosphorylation of p65 on serine 536 [58]. Moreover, TNF-α overproduction has been involved in the onset of multiple illnesses, including cancer. Current research have developed to identify promising compounds as TNF-α pathway inhibitors [59]. In this finding, the phosphorylation of IκBα and p65 stimulated by TNF-α exposure were suppressed by ampelopsin pretreatment, suggesting that ampelopsin has important ability to inhibit the TNF-α/NF-κB axis

in resistant cells. It is necessary to develop further experiment to investigate the underlying mechanism how NF-κB controls cancer stem cell properties and OXPHOS metabolism in breast CSCs.

5. CONCLUSIONS

Ampelopsin, a primary component found in Ampelopsis species, is previous reported to have anticancer ability. To the best of our knowledge, this is first time to determine a crucial role of ampelopsin in suppressing proliferation and triggering apoptosis in triple neagative chemo- and radio-resistant breast cancer cells. Remakably, ampelopsin diminished stemness charateristics and OXPHOS metabolism in MDA-MB-231/IR cells. Moreover, the enrichment of NF-κB signaling in these cells was also inhibited by ampelopsin, implying a potential chemotherapeutic agent modulating CSC phenotype in TNBC treatment.

SUPPLEMENTARY DATA

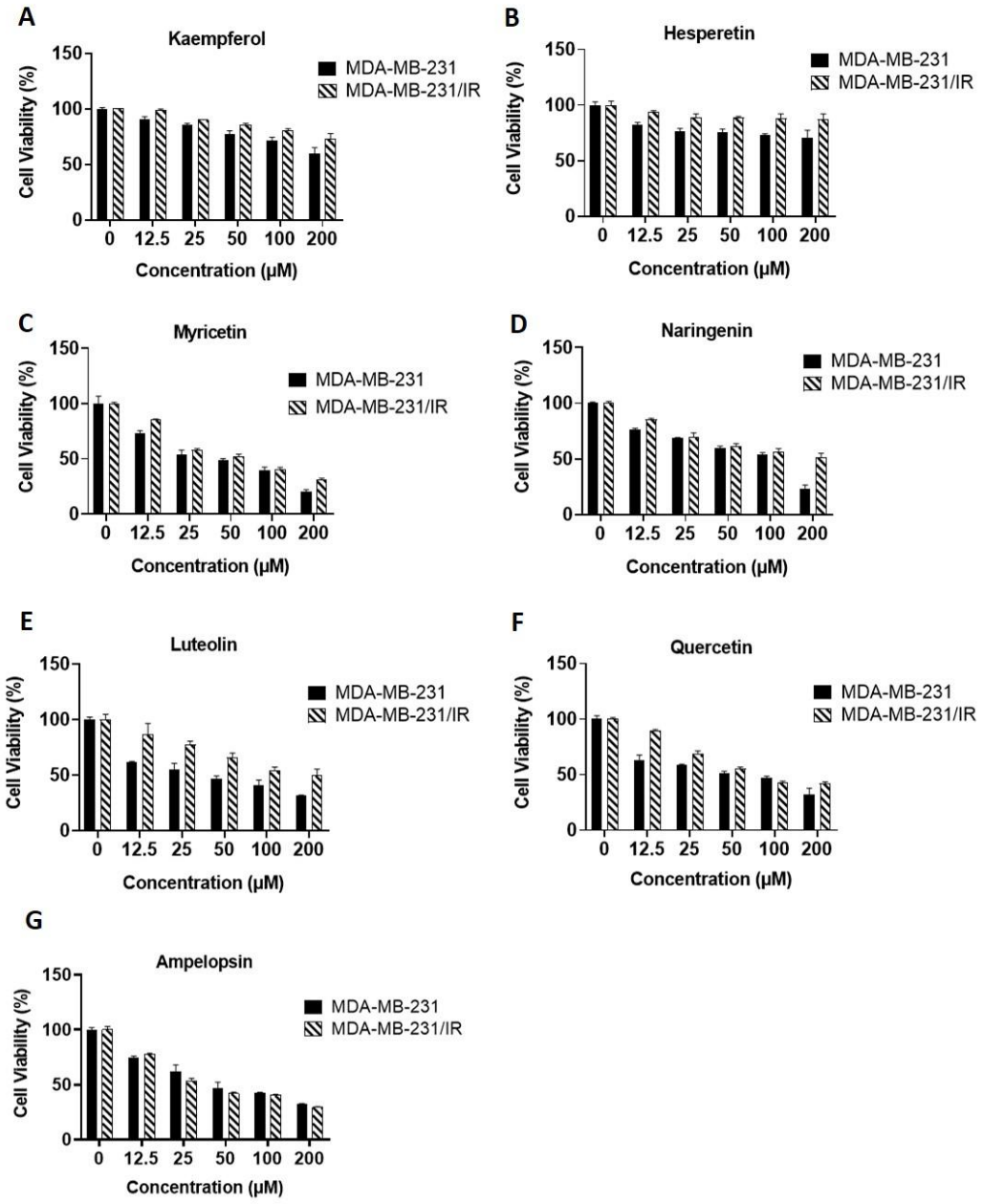

Fig. S1. Flavonoid compounds targets cell viability of MDA-MB-231 and MDA-MB-231/IR cells.

Effects on cell viability of incubation for 24 h with (A) kaempferol, (B) hesperetin, (C) myricetin, (D) naringenin, (E) luteolin, (F) quercetin and (G) ampelopsin were evaluated by

MTT assay. Only ampelopsin had higher cytotoxicity in MDA-MB-231/IR cells rather than in MDA-MB-231 cells.

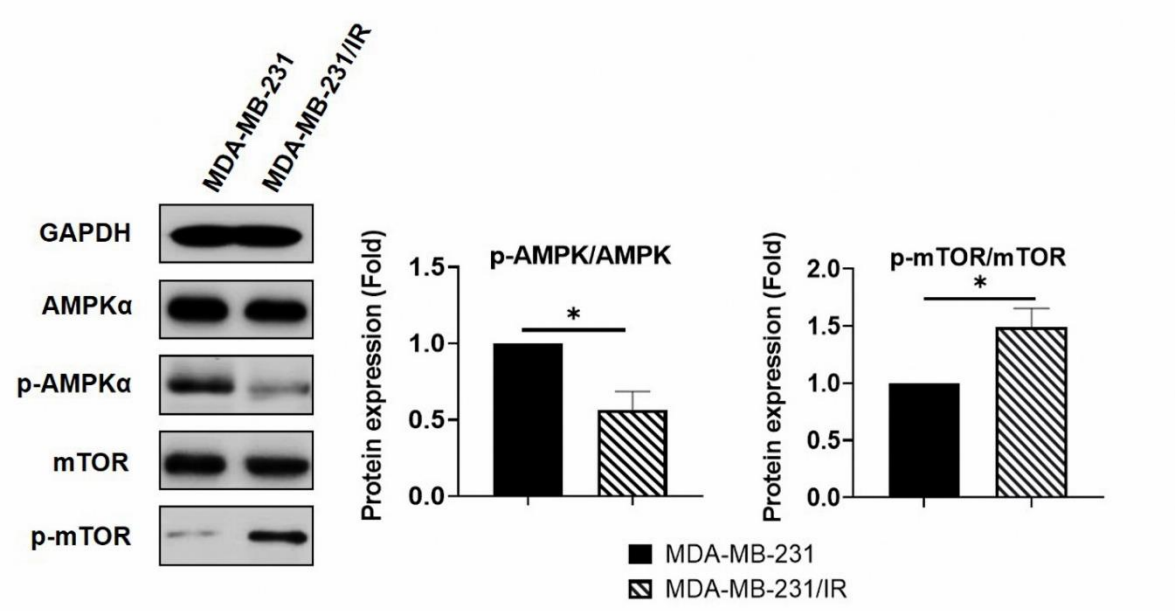

Fig. S2. The levels of AMPK, p-AMPK, mTOR and p-mTOR were evaluated in MDA-MB-231 and MDA-MB-231/IR cells.

By Western blotting analysis, MDA-MB-231/IR cells showed reduced AMPK activation and increased mTOR phosphorylation, compared with MDA-MB-231 cells. GAPDH was considered as a control.

Table S1. The sequences of primers for mitochondrial OXPHOS genes.

Gene	Primer sequences
NDUFA10	5′-CACCTGCGATTACTGGTTCAG-3′ 5′-GCAGCTCTCTGAACTGATGTA-3′
SDHB	5′-AGCCTTATCTGAAGAAGAAGG-3′ 5′-TACTTGTCTCCGTTCCACCAG-3′
COX5B	5′-CAGAAGGGACTGGACCCATA-3′ 5′-TTCACAGATGCAGCCCACTA-3′
COX4I1	5′-ACGAGCTCATGAAAGTGTTGTG-3′ 5′-AATGCGATACAACTCGACTTTCTC-3′
ATP5G3	5′-GGATTTGCCTTGTCTGAAGC-3′ 5′-CGTACATTCCCATGACACCA-3′
SCO2	5′-TGGGTGCTGATGTACTTTGGC-3′ 5′-ACAGTCTTGGGTGGAAGTCCTG-3′
CYC1	5′-TAGAGTTTGACGATGGCACCC-3′ 5′-CGTTTTCGATGGTCGTGCTC-3′
UQCRC1	5′-ACGGTGGGAGTGTGGATTGAC-3′ 5′-CATTGCCAGGCCGATTCTTTG-3′
ATP5B	5′-GGCACAATGCAGGAAAGG-3′ 5′-TCGGCAGGCACATAGATAGCC-3′
PGC1-α	5′-TTCCACCAAGAGCAAGTAT-3′ 5′-CGCTGTCCCATGAGGTATT-3′

REFERENCES

1. Sung, H.; Ferlay, J.; Siegel, R.L.; Laversanne, M.; Soerjomataram, I.; Jemal, A.; Bray, F. Global cancer statistics 2020: GLOBOCAN estimates of incidence and mortality worldwide for 36 cancers in 185 countries. *CA Cancer J. Clin.* **2021**.
2. Sun, X.; Wang, M.; Wang, M.; Yu, X.; Guo, J.; Sun, T.; Li, X.; Yao, L.; Dong, H.; Xu, Y. Metabolic reprogramming in triple-negative breast cancer. *Front. Oncol.* **2020**, *10*, p. 428.
3. Yin, L.; Duan, J.-J.; Bian, X.-W.; Yu, S.-c. Triple-negative breast cancer molecular subtyping and treatment progress. *Breast Cancer Res.* **2020**, *22*, 1-13.
4. Park, S.Y.; Choi, J.H.; Nam, J.S. Targeting Cancer Stem Cells in Triple-Negative Breast Cancer. *Cancers (Basel)* **2019**, *11*.
5. Butti, R.; Gunasekaran, V.P.; Kumar, T.V.; Banerjee, P.; Kundu, G.C. Breast cancer stem cells: Biology and therapeutic implications. *Int. J. Biochem. Cell Biol.* **2019**, *107*, 38-52, doi: .
6. Yang, L.; Shi, P.; Zhao, G.; Xu, J.; Peng, W.; Zhang, J.; Zhang, G.; Wang, X.; Dong, Z.; Chen, F. Targeting cancer stem cell pathways for cancer therapy. *Signal Transduct Target Ther* **2020**, *5*, 1-35.
7. Koh, S.Y.; Moon, J.Y.; Unno, T.; Cho, S.K. Baicalein suppresses stem cell-like characteristics in radio-and chemoresistant MDA-MB-231 human breast cancer cells through up-regulation of IFIT2. *Nutrients* **2019**, *11*, 624.
8. Nguyen, Y.T.-K.; Moon, J.Y.; Ediriweera, M.K.; Cho, S.K. Phenethyl isothiocyanate suppresses stemness in the chemo-and radio-resistant triple-negative breast cancer cell line MDA-MB-231/IR via downregulation of metadherin. *Cancers* **2020**, *12*, 268.
9. Snyder, V.; Reed-Newman, T.C.; Arnold, L.; Thomas, S.M.; Anant, S. Cancer Stem Cell Metabolism and Potential Therapeutic Targets. *Front. Oncol.* **2018**, *8*, 203.

10. Hanahan, D.; Weinberg, Robert A. Hallmarks of Cancer: The Next Generation. *Cell* **2011**, *144*, 646-674, doi:10.1016/j.cell.2011.02.013.

11. Valle, S.; Alcalá, S.; Martin-Hijano, L.; Cabezas-Sáinz, P.; Navarro, D.; Muñoz, E.R.; Yuste, L.; Tiwary, K.; Walter, K.; Ruiz-Cañas, L. Exploiting oxidative phosphorylation to promote the stem and immunoevasive properties of pancreatic cancer stem cells. *Nat. Commun.* **2020**, *11*, 1-19.

12. Liu, G.; Luo, Q.; Li, H.; Liu, Q.; Ju, Y.; Song, G. Increased oxidative phosphorylation is required for stemness maintenance in liver cancer stem cells from hepatocellular carcinoma cell line HCCLM3 cells. *Int. J. Mol. Sci.* **2020**, *21*, 5276.

13. Mauro, C.; Leow, S.C.; Anso, E.; Rocha, S.; Thotakura, A.K.; Tornatore, L.; Moretti, M.; De Smaele, E.; Beg, A.A.; Tergaonkar, V. NF-κB controls energy homeostasis and metabolic adaptation by upregulating mitochondrial respiration. *Nat. Cell Biol.* **2011**, *13*, 1272-1279.

14. Sica, V.; Bravo-San Pedro, J.M.; Stoll, G.; Kroemer, G. Oxidative phosphorylation as a potential therapeutic target for cancer therapy. *Int. J. Cancer* **2020**, *146*, 10-17.

15. Wang, W.; Nag, S.A.; Zhang, R. Targeting the NFκB signaling pathways for breast cancer prevention and therapy. *Curr. Med. Chem.* **2015**, *22*, 264-289.

16. Rinkenbaugh, A.L.; Baldwin, A.S. The NF-κB Pathway and Cancer Stem Cells. *Cells* **2016**, *5*.

17. Giridharan, S.; Srinivasan, M. Mechanisms of NF-κB p65 and strategies for therapeutic manipulation. *J. Inflamm. Res.* **2018**, *11*, 407-419.

18. Gao, Y.; Yang, Y.; Yuan, F.; Huang, J.; Xu, W.; Mao, B.; Yuan, Z.; Bi, W. TNFα-YAP/p65-HK2 axis mediates breast cancer cell migration. *Oncogenesis* **2017**, *6*, e383-e383.

19. Wang, L.; Kang, F.; Li, J.; Zhang, J.; Shan, B. Overexpression of p65 attenuates celecoxib-induced cell death in MDA-MB-231 human breast cancer cell line. *Cancer Cell Int.* **2013**, *13*, 1-9.

20. Lu, X.; An, H.; Jin, R.; Zou, M.; Guo, Y.; Su, P.; Liu, D.; Shyr, Y.; Yarbrough, W. PPM1A is a RelA phosphatase with tumor suppressor-like activity. *Oncogene* **2014**, *33*, 2918-2927.

21. Christian, F.; Smith, E.L.; Carmody, R.J. The Regulation of NF-κB Subunits by Phosphorylation. *Cells* **2016**, *5*.

22. Ashraf, M.A. Phytochemicals as Potential Anticancer Drugs: Time to Ponder Nature's Bounty. *Biomed Res. Int.* **2020**, *2020*, 8602879.

23. Zhang, Y.; Que, S.; Yang, X.; Wang, B.; Qiao, L.; Zhao, Y. Isolation and identification of metabolites from dihydromyricetin. *Magn Reson Chem* **2007**, *45*, 909-916.

24. Hyun, T.K.; Eom, S.H.; Yu, C.Y.; Roitsch, T. Hovenia dulcis–an Asian traditional herb. *Planta Med.* **2010**, *76*, 943-949.

25. Liu, D.; Mao, Y.; Ding, L.; Zeng, X.-A. Dihydromyricetin: A review on identification and quantification methods, biological activities, chemical stability, metabolism and approaches to enhance its bioavailability. *Trends Food Sci. Technol.* **2019**, *91*, 586-597.

26. Zhang, J.; Chen, Y.; Luo, H.; Sun, L.; Xu, M.; Yu, J.; Zhou, Q.; Meng, G.; Yang, S. Recent update on the pharmacological effects and mechanisms of dihydromyricetin. *Front. Pharmacol.* **2018**, *9*, 1204.

27. Xu, Y.; Wang, S.; Chan, H.F.; Lu, H.; Lin, Z.; He, C.; Chen, M. Dihydromyricetin Induces Apoptosis and Reverses Drug Resistance in Ovarian Cancer Cells by p53-mediated Downregulation of Survivin. *Sci. Rep.* **2017**, *7*, 46060.

28. Tong, H.; Zhang, X.; Tan, L.; Jin, R.; Huang, S.; Li, X. Multitarget and promising role of dihydromyricetin in the treatment of metabolic diseases. *Eur. J. Pharmacol.* **2020**, *870*, 172888.

29. To, N.B.; Nguyen, Y.T.-K.; Moon, J.Y.; Ediriweera, M.K.; Cho, S.K. Pentadecanoic Acid, an Odd-Chain Fatty Acid, Suppresses the Stemness of MCF-7/SC Human Breast Cancer Stem-Like Cells through JAK2/STAT3 Signaling. *Nutrients* **2020**, *12*, 1663.

30. Livak, K.J.; Schmittgen, T.D. Analysis of relative gene expression data using real-time quantitative PCR and the 2− ΔΔCT method. *Methods.* **2001**, *25*, 402-408.

31. Hyun, H.B.; Moon, J.Y.; Cho, S.K. Quercetin suppresses cyr61-mediated multidrug resistance in human gastric adenocarcinoma ags cells. *Molecules* **2018**, *23*, 209.

32. Kim, S.-H.; Hwang, K.-A.; Choi, K.-C. Treatment with kaempferol suppresses breast cancer cell growth caused by estrogen and triclosan in cellular and xenograft breast cancer models. *J. Nutr. Biochem.* **2016**, *28*, 70-82.

33. Palit, S.; Kar, S.; Sharma, G.; Das, P.K. Hesperetin induces apoptosis in breast carcinoma by triggering accumulation of ROS and activation of ASK1/JNK pathway. *J. Cell. Physiol.* **2015**, *230*, 1729-1739.

34. Knickle, A.; Fernando, W.; Greenshields, A.L.; Rupasinghe, H.V.; Hoskin, D.W. Myricetin-induced apoptosis of triple-negative breast cancer cells is mediated by the iron-dependent generation of reactive oxygen species from hydrogen peroxide. *Food Chem. Toxicol.* **2018**, *118*, 154-167.

35. Zhao, Z.; Jin, G.; Ge, Y.; Guo, Z. Naringenin inhibits migration of breast cancer cells via inflammatory and apoptosis cell signaling pathways. *Inflammopharmacology* **2019**, *27*, 1021-1036.

36. Huang, L.; Jin, K.; Lan, H. Luteolin inhibits cell cycle progression and induces apoptosis of breast cancer cells through downregulation of human telomerase reverse transcriptase. *Oncol. Lett.* **2019**, *17*, 3842-3850.

37. Chien, S.-Y.; Wu, Y.-C.; Chung, J.-G.; Yang, J.-S.; Lu, H.-F.; Tsou, M.-F.; Wood, W.; Kuo, S.-J.; Chen, D.-R. Quercetin-induced apoptosis acts through mitochondrial- and caspase-3-dependent pathways in human breast cancer MDA-MB-231 cells. *Hum Exp Toxicol* **2009**, *28*, 493-503.

38. Yu, S.W.; Andrabi, S.A.; Wang, H.; Kim, N.S.; Poirier, G.G.; Dawson, T.M.; Dawson, V.L. Apoptosis-inducing factor mediates poly(ADP-ribose) (PAR) polymer-induced cell death. *Proc. Natl. Acad. Sci. U.S.A.* **2006**, *103*, 18314-18319.

39. Kaufmann, S.H.; Desnoyers, S.; Ottaviano, Y.; Davidson, N.E.; Poirier, G.G. Specific proteolytic cleavage of poly (ADP-ribose) polymerase: an early marker of chemotherapy-induced apoptosis. *Cancer Res.* **1993**, *53*, 3976-3985.

40. Lundholm, L.; Hååg, P.; Zong, D.; Juntti, T.; Mörk, B.; Lewensohn, R.; Viktorsson, K. Resistance to DNA-damaging treatment in non-small cell lung cancer tumor-initiating cells involves reduced DNA-PK/ATM activation and diminished cell cycle arrest. *Cell Death Dis.* **2013**, *4*, e478-e478.

41. O'Brien, C.A.; Kreso, A.; Jamieson, C.H. Cancer stem cells and self-renewal. *Clin. Cancer Res.* **2010**, *16*, 3113-3120.

42. Luo, M.; Brooks, M.; Wicha, M.S. Epithelial-mesenchymal plasticity of breast cancer stem cells: implications for metastasis and therapeutic resistance. *Curr. Pharm. Des.* **2015**, *21*, 1301-1310.

43. Gao, H.; Liang, D.; Li, C.; Xu, G.; Jiang, M.; Li, H.; Yin, J.; Song, Y. 2-Deoxy-Rh2: A novel ginsenoside derivative, as dual-targeting anti-cancer agent via regulating apoptosis and glycolysis. *Biomed. Pharmacother.* **2020**, *124*, 109891.

44. Wu, Y.; Zhou, B.P. TNF-alpha/NF-kappaB/Snail pathway in cancer cell migration and invasion. *Br. J. Cancer* **2010**, *102*, 639-644.

45. Xia, J.; Guo, S.; Fang, T.; Feng, D.; Zhang, X.; Zhang, Q.; Liu, J.; Liu, B.; Li, M.; Zhu, R. Dihydromyricetin induces autophagy in HepG2 cells involved in inhibition of mTOR and regulating its upstream pathways. *Food Chem. Toxicol.* **2014**, *66*, 7-13.

46. Guo, Z.; Guozhang, H.; Wang, H.; Li, Z.; Liu, N. Ampelopsin inhibits human glioma through inducing apoptosis and autophagy dependent on ROS generation and JNK pathway. *Biomed. Pharmacother.* **2019**, *116*, 108524.

47. Yu, F.; Li, J.; Chen, H.; Fu, J.; Ray, S.; Huang, S.; Zheng, H.; Ai, W. Kruppel-like factor 4 (KLF4) is required for maintenance of breast cancer stem cells and for cell migration and invasion. *Oncogene* **2011**, *30*, 2161-2172.

48. Zhang, Y.; Wang, X. Targeting the Wnt/β-catenin signaling pathway in cancer. *J. Hematol. Oncol.* **2020**, *13*, 1-16.

49. Hong, D.; Fritz, A.J.; Zaidi, S.K.; van Wijnen, A.J.; Nickerson, J.A.; Imbalzano, A.N.; Lian, J.B.; Stein, J.L.; Stein, G.S. Epithelial-to-mesenchymal transition and cancer stem cells contribute to breast cancer heterogeneity. *J. Cell. Physiol.* **2018**, *233*, 9136-9144.

50. Li, W.; Saud, S.M.; Young, M.R.; Chen, G.; Hua, B. Targeting AMPK for cancer prevention and treatment. *Oncotarget* **2015**, *6*, 7365-7378.

51. Xiang, H.-C.; Lin, L.-X.; Hu, X.-F.; Zhu, H.; Li, H.-P.; Zhang, R.-Y.; Hu, L.; Liu, W.-T.; Zhao, Y.-L.; Shu, Y. AMPK activation attenuates inflammatory pain through inhibiting NF-κB activation and IL-1β expression. *J. Neuroinflammation* **2019**, *16*, 1-12.

52. Dong, L.-x.; Sun, L.-l.; Zhang, X.; Pan, L.; Lian, L.-j.; Chen, Z.; Zhong, D.-s. Negative regulation of mTOR activity by LKB1-AMPK signaling in non-small cell lung cancer cells. *Acta Pharmacol. Sin.* **2013**, *34*, 314-318.

53. Silva, J.; Yu, X.; Moradian, R.; Folk, C.; Spatz, M.H.; Kim, P.; Bhatti, A.A.; Davies, D.L.; Liang, J. Dihydromyricetin protects the liver via changes in lipid metabolism and enhanced ethanol metabolism. *Alcohol. Clin. Exp. Res.* **2020**, *44*, 1046-1060.

54. Kim, I.; Kim, M.; Park, M.K.; Naik, R.; Park, J.H.; Kim, B.-K.; Choi, Y.; Chang, K.Y.; Won, M.; Ban, H.S. The disubstituted adamantyl derivative LW1564 inhibits the growth of cancer cells by targeting mitochondrial respiration and reducing hypoxia-inducible factor (HIF)-1α accumulation. *Exp. Mol. Med.* **2020**, 1-12.

55. Motolani, A.; Martin, M.; Sun, M.; Lu, T. Phosphorylation of the Regulators, a Complex Facet of NF-κB Signaling in Cancer. *Biomolecules* **2021**, *11*, 15.

56. Chen, L.-F.; Greene, W.C. Shaping the nuclear action of NF-κB. *Nat. Rev. Mol. Cell Biol.* **2004**, *5*, 392-401.

57. Capece, D.; Verzella, D.; Di Francesco, B.; Alesse, E.; Franzoso, G.; Zazzeroni, F. NF-κB and mitochondria cross paths in cancer: mitochondrial metabolism and beyond. In Proceedings of the Semin. Cell Dev. Biol., 2020; pp. 118-128.

58. Sakurai, H.; Suzuki, S.; Kawasaki, N.; Nakano, H.; Okazaki, T.; Chino, A.; Doi, T.; Saiki, I. Tumor necrosis factor-α-induced IKK phosphorylation of NF-κB p65 on serine 536 is mediated through the TRAF2, TRAF5, and TAK1 signaling pathway. *J. Biol. Chem.* **2003**, *278*, 36916-36923.

59. Iqbal, M.; Verpoorte, R.; Korthout, H.A.A.J.; Mustafa, N.R. Phytochemicals as a potential source for TNF-α inhibitors. *Phytochem Rev* **2013**, *12*, 65-93.